

Implications of neurovascular uncoupling in functional magnetic resonance imaging (fMRI) of brain tumors

Rebecca W Pak¹, Darian H Hadjiabadi¹, Janaka Senarathna¹,
Shruti Agarwal², Nitish V Thakor¹, Jay J Pillai^{2,*} and
Arvind P Pathak^{1,2,3,*}

Abstract

Functional magnetic resonance imaging (fMRI) serves as a critical tool for presurgical mapping of eloquent cortex and changes in neurological function in patients diagnosed with brain tumors. However, the blood-oxygen-level-dependent (BOLD) contrast mechanism underlying fMRI assumes that neurovascular coupling remains intact during brain tumor progression, and that measured changes in cerebral blood flow (CBF) are correlated with neuronal function. Recent preclinical and clinical studies have demonstrated that even low-grade brain tumors can exhibit neurovascular uncoupling (NVU), which can confound interpretation of fMRI data. Therefore, to avoid neurosurgical complications, it is crucial to understand the biophysical basis of NVU and its impact on fMRI. Here we review the physiology of the neurovascular unit, how it is remodeled, and functionally altered by brain cancer cells. We first discuss the latest findings about the components of the neurovascular unit. Next, we synthesize results from preclinical and clinical studies to illustrate how brain tumor induced NVU affects fMRI data interpretation. We examine advances in functional imaging methods that permit the clinical evaluation of brain tumors with NVU. Finally, we discuss how the suppression of anomalous tumor blood vessel formation with antiangiogenic therapies can “normalize” the brain tumor vasculature, and potentially restore neurovascular coupling.

Keywords

Neurovascular, coupling, functional magnetic resonance imaging, cancer, angiogenesis, cooption

Received 13 December 2016; Revised 22 March 2017; Accepted 30 March 2017

Neurovascular coupling is the relationship between neural firing and concomitant changes in cerebral blood flow to accommodate changing energy demands.^{1,2} This relationship constitutes the basis of the blood-oxygen-level-dependent (BOLD) contrast mechanism that underlies functional magnetic resonance imaging (fMRI) of the brain. However, the BOLD signal is not perfectly correlated with neuronal action potentials. The BOLD signal is a mixture of several phenomena including changes in cerebral blood flow (CBF), cerebral blood volume (CBV), and the cerebral metabolic rate for oxygen consumption (CMRO₂).³ Nonetheless, it is this neurovascular coupling that has made fMRI the workhorse for interrogating and mapping brain function in patients.⁴

¹Department of Biomedical Engineering, The Johns Hopkins University School of Medicine, Baltimore, USA

²Russell H. Morgan Department of Radiology and Radiological Science, The Johns Hopkins University School of Medicine, Baltimore, USA

³Sidney Kimmel Comprehensive Cancer Center, The Johns Hopkins University School of Medicine, Baltimore, USA

*Co-senior authors.

Corresponding author:

Arvind P Pathak, Division of Cancer Imaging Research, Russell H. Morgan Department of Radiology and Radiological Science, The Johns Hopkins University School of Medicine, 720 Rutland Avenue, 217 Traylor Bldg., Baltimore, MD 21205, USA.
Email: pathak@mri.jhu.edu

More recently, fMRI studies using low frequency fluctuations of the BOLD signal acquired from the “resting state” (rs-fMRI) have also successfully mapped resting-state brain connectivity⁵ on the basis of this underlying neurovascular coupling. However, recent preclinical and clinical studies have demonstrated that brain tumors can exhibit NVU that can confound the interpretation of fMRI data.⁶ Therefore, before one can exploit fMRI signals as biomarkers of diseases involving the neurovasculature (e.g. brain tumors and stroke), one needs to gain an appreciation of how neurovascular coupling is affected by different diseases. Specifically, one must first familiarize oneself with the architecture of the healthy “neurovascular unit.”

The neurovascular unit in homeostasis

Over a century ago, Roy and Sherrington described neurovascular coupling as the mechanism by which neuronal activity influenced cerebral blood flow.² When stimulating regions such as the medulla oblongata, they observed vasoconstriction in other organs and increases in arterial pressure that brought blood to the stimulated region.² Around the same time while many researchers were focused on the study of the electrical activity of neurons, Cajal suggested the importance of neuroglia, particularly astrocytes, in neurovascular coupling.⁷ Counter to the prevailing idea of the time that astrocytes served only as structural support cells, Cajal proposed the *insulation theory* in which astrocytes served as barriers between neighboring neurons.⁸ More recently, astrocytes have emerged as key

players in the communication between cerebral blood vessels and neurons in conjunction with other components of the neurovascular unit.⁹

The neurovascular unit is comprised of three fundamental cell types: astrocytes, pericytes, and endothelial cells (Figure 1). A number of recent studies have demonstrated the role of astrocytic endfeet in the homeostatic functioning of the brain.¹⁰ Astrocytes facilitate neurovascular coupling by releasing vasoactive molecules that regulate the tone of vascular smooth muscle cells (VSMCs) and contribute to vasodilation in activated brain regions. Such vasodilation results in increases in regional CBF to satisfy the increasing energy demands of active neurons.¹¹ Astrocytes also produce arachidonic acid (AA) that facilitates vasoconstriction.¹² In addition, astrocytes are responsible for holding together tight junctions that constitute the blood–brain barrier (BBB).¹³ In the absence of intact tight junctions, the neurovasculature becomes leaky and the BBB is breached, allowing for pathogens and hydrophilic molecules to enter the brain parenchyma, as is often observed in patients with infections or brain cancer.¹⁴

In addition to astrocytes, pericytes also contribute to healthy neurovascular coupling.¹⁵ During development, pericytes are thought to be involved in tight junction and blood vessel formation.¹⁶ This includes BBB formation during which they regulate permeability of vessels and immune cell passage.¹¹ In addition, pericyte signaling pathways inhibit endothelial cell proliferation and promote their maturation into healthy blood vessels.¹⁶ Overall, studies have shown that pericytes are

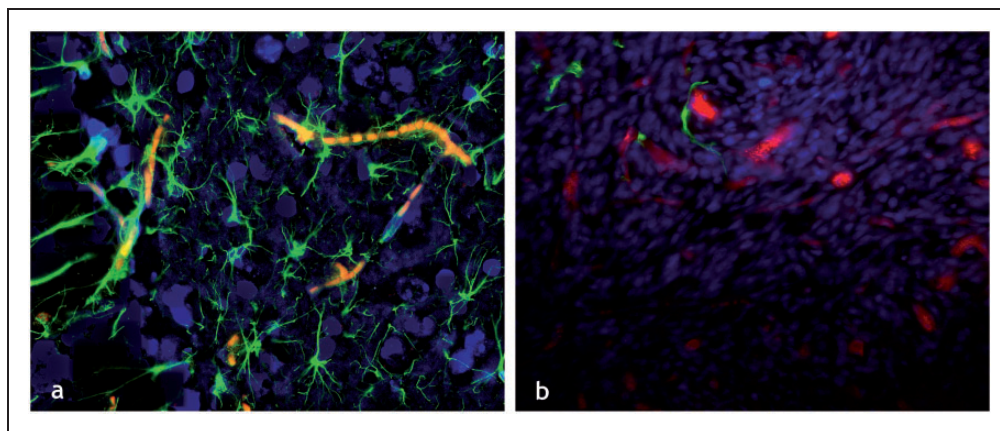


Figure 1. The healthy and cancer-disrupted neurovascular unit: Immunofluorescently labeled elements of (a) the healthy neurovascular unit in a tissue section from a murine brain showing GFAP labeled astrocytes (green channel), DAPI labeled cell nuclei (blue channel), and autofluorescing erythrocytes or RBCs (red channel). The dense vascular coverage of the astrocytes is immediately apparent as is the intimate contact between the astrocytic endfeet and neurovascular endothelium. (b) Disrupted neurovascular unit in a 9L brain tumor bearing murine brain section, wherein one can not only see a dearth of astrocytic coverage (green channel) of the tumor vessels (dextran-TRITC label in red channel) but also displaced astrocytic endfeet. All images were acquired at 20× magnification.

involved in mechanisms that ensure the formation of normal blood vessels and suppression of malformed ones.¹⁷

Together, astrocytes and pericytes were thought to be the primary mediators of neurovascular coupling and stabilization of the BBB. However, recent evidence from Chen et al. suggested that vascular endothelial cells may also play a role in the neurovascular coupling mechanism.¹⁸ In their study, they injected a fluorescent dye into the vessels and used a laser light at the dye's excitation wavelength to generate reactive oxygen species (ROS).¹⁸ These dye-generated ROS molecules disrupted endothelial cell membranes, preventing downstream endothelial cell signaling, namely the retrograde dilation of pial arteries in response to hyperemia.^{18,19} Before light-dye treatment, stimulation was observed to cause pial artery dilation.¹⁸ However, after light-dye treatment, dilation appeared to be blocked and pial artery diameters remained unchanged¹⁸ (Figure 2). This experiment suggested that NVU occurs when endothelial cells do not function properly. In addition, the authors reported that the hemodynamic response could be classified as fast or slow vasodilations.^{18,20} Fast vasodilation occurs as a result of membrane hyperpolarization and has a more global effect, whereas the slow type occurs locally due to movement of calcium ions (Ca^{2+}).^{18,20} The initial peak of the hemodynamic response was lost with endothelial disruption.¹⁸ Therefore, the endothelium appeared to facilitate healthy neurovascular function and its fast response appeared to be attenuated with cell membrane disruption. Finally, a brain-wide paravascular pathway for clearing extracellular proteins was recently identified in lieu of a lymphatic system.²¹ Since this pathway operates via glial water flux and plays a role akin to the lymphatic system, it has been dubbed

the “glymphatic” system of the brain. Recent research suggested that this glymphatic coupling with cerebral blood flow may also contribute to the health of the neurovascular unit by providing a method for clearing waste products from the brain. While the role of this new pathway in different neuropathologies is only just emerging,²² its potential role in NVU remains to be elucidated.

The vasculature of brain tumors

Glioma cells are able to initially grow around pre-existing vessels forming cuff-like clusters through a mechanism dubbed vascular co-option²³ and can then induce new vasculature via de novo angiogenesis.²⁴ Glioma growth often begins with co-option, invading the perivascular space to create satellite tumors.^{23,25} With the increasing energy demands of progressing tumors, some of these original host vessels may undergo apoptosis. During this process of cell death, vascular endothelial growth factor (VEGF) is released, which eventually promotes robust angiogenesis to rescue tumor growth.²³ Poor brain tumor perfusion often results in a paucity of oxygen and other blood-borne molecules, often leading to a hypoxic tumor microenvironment. Hypoxia causes an increase in angiopoietin-2 (ANG-2), which together with VEGF leads to the sprouting of new vessels²⁶ accompanied by the migration and proliferation of endothelial cells.²⁷ Hypoxia and increased ANG-2 concentrations also lead to an increase in hypoxia-inducible factors (HIFs), which further upregulate VEGF.²⁸ High levels of VEGF can cause increases in brain-derived neurotrophic factor (BDNF), which has been shown to play a dynamic role during vascular development, maintenance of the cerebrovascular

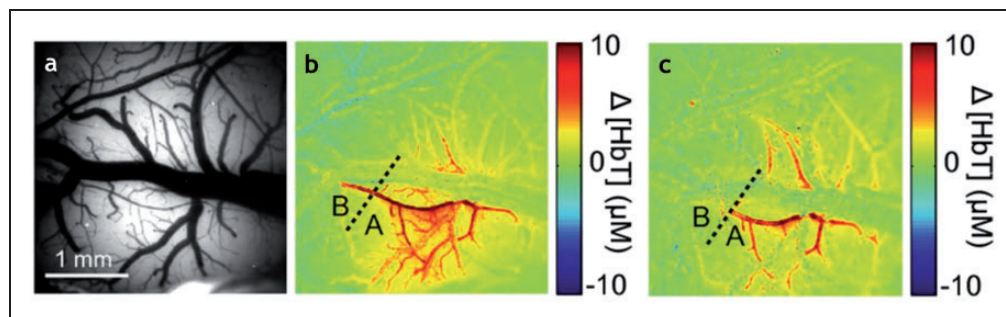


Figure 2. The emergent role of the endothelium in neurovascular uncoupling: Perfusion of blood vessels before and after light dye treatment. Before the light treatment, vasculature was (a) illuminated by 534 nm light, and (b) a map of the total hemoglobin (ΔHbT) constructed, clearly indicating blood flow in the vessels. The light-dye method selectively disrupted endothelial cells, so treatment (c) reduced dilation in the pial arteries, as demonstrated by the significantly decreased levels of ΔHbT . This absence of vascular response after endothelial disruption suggested that the endothelium plays an essential role in neurovascular coupling. Adapted with permission from Hillman et al.²⁰

endothelium and the interplay between angiogenesis and neurogenesis.^{23,29,30}

In healthy individuals, angiopoietin-1 (ANG-1) and ANG-2 act as antagonists although both can be pro- and anti-angiogenic. Thus, the elevated ANG-2 in hypoxic environments offsets the balance of these two molecules.^{28,31} ANG-1 is responsible for pericyte recruitment, which is important for maintaining blood vessel integrity.³² Furthermore, the binding of ANG-2 to its receptor, TIE-2, disrupts tight endothelial cell junctions and can result in a compromised BBB.^{25,32} Breaching the BBB can lead to a number of complications such as vasogenic edema.³³ Due to the confines of the skull, the volume of the brain is limited. Thus, with fluid leakage from the BBB, interstitial fluid pressure (IFP) in the tumor rises as fluid accumulates in the brain.^{34,35} As a consequence of increasing IFP, cerebrospinal fluid (CSF) pressure also rises until it equilibrates. This elevated IFP remains an obstacle for drug delivery in brain tumors.³⁶ Furthermore, edema has a tendency to occur along white matter tracts,³⁷ leading to possible disruption of connectivity between brain regions. Moreover, VEGF, which likely contributes to BBB hyperpermeability, is also a chemoattractant for macrophages that can lead to further pathogenesis.³⁴

Glioma cells are also able to grow by vasculogenesis, a process in which bone-marrow-derived cells (BMDC) are recruited through the circulatory system and incorporated into new vasculature.^{28,38} New endothelial cells can also be formed via the differentiation of tumor-associated macrophages (TAMs) as well as glioblastoma stem cells (GSCs).³⁹ High levels of VEGF from angiogenic mechanisms may also lead to an increase in neural stem cells (NSCs)⁴⁰ that encourage cell migration and neuronal differentiation.^{41,42} Although the frequency of vasculogenesis in glioblastoma (GBM) is still being debated, it has the potential to contribute to anti-angiogenic therapy resistance and progression of GBM.^{39,43} Finally, tumor cells may also use "intussusception" to proliferate.^{44,45} Intussusceptive angiogenesis is a process in which interstitial tissue columns protrude into the lumen of a preexisting vessel and split it in two, thereby remodeling the cerebrovasculature.⁴⁵ These chemical and physical alterations in the cellular microenvironment in the presence of GBM also cause functional and structural changes in the neurovascular unit, as discussed in the next section.

Brain tumors alter the neurovascular unit

NVU has been implicated in a number of neurodegenerative diseases including stroke, Alzheimer's and Parkinson's disease.⁴⁶ NVU has also been observed in brain tumors⁴⁷ and is now being investigated from

a mechanistic perspective. A recent histopathological study by Lee et al. elegantly demonstrated that gliomas can invade the perivascular space and disrupt the normal interactions between the astrocytes, pericytes, and endothelial cells as described in the ensuing paragraphs.¹⁴

Aquaporin-4 (AQP4) is a highly expressed water channel in astrocytes that enables their polarization. These channels normally cover the contact area between the glial cell membrane and the mesenchymal space.⁴⁸ However, in GBM, this spatial specificity is lost and AQP4 is distributed all over the cell surface.⁴⁸⁻⁵⁰ This change in location of AQP4 is thought to contribute to the functional damage observed in GBM patients.⁵¹

By simultaneously staining VSMCs and astrocytes in brain tumor bearing tissue sections, the Sontheimer group localized astrocytes relative to the vasculature, namely around arteries and capillaries.¹¹ Healthy brain vessels were surrounded by astrocytes (similar to Figure 1(a)), whereas those invaded by glioma cells had astrocytes dissociated or absent from the vasculature (similar to Figure 1(b)). They also showed that in addition to the displacement of the astrocytic endfeet, glioma cells took over the areas surrounding blood vessels, particularly favoring small capillaries.¹¹ Their study suggested that in conjunction, these two effects prevented vasoactive molecules released by astrocytes from reaching the endothelial cells.¹¹ This attenuated the cerebrovascular response to neuronal activity even though VSMCs could still be responsive to these vasoactive molecules.¹¹ Studies from our laboratory in pre-clinical brain tumor models have demonstrated a similar paucity of astrocyte coverage for brain tumor vasculature (Figure 1(b)). Moreover, recent work by Chen et al. directly implicated the role of endothelial cells in neurovascular coupling, positing that endothelial dysfunction alone could result in NVU without any concomitant changes in adjacent astrocytes and/or the presence of tumor cells.¹⁸

More recently, elegant studies with multiphoton microscopy have revealed that the growth and proliferation of a few or even a single glioma cell can cause NVU.¹¹ Invading glioma cells lead to NVU and can also hijack the extant vasculature and take control of vascular tone. Using Ca²⁺-activated K⁺ channels, which are highly expressed in GBM, glioma cells change K⁺ concentrations to alter the blood vessel diameter.¹¹ Furthermore, glioma cells may increase their invasion area in the perivascular space by inducing vasoconstriction.¹¹

It has also been suggested that the inability to deliver the metabolites required for neural firing may lead to faster excitotoxicity.¹¹ In addition to uncoupling, the growth of glioma cells on the abluminal surface of the

cerebrovasculature and the disruption of astrocyte function likely compromise the tight junctions of the BBB. Together with the down-regulation of tight junction proteins (claudin-1,-3, and -5), gliomas open the BBB.⁵² This creates leaky blood vessels and activates pro-inflammatory responses.⁵² Finally, glioma growth on the abluminal surface of blood vessels displaces encasing pericytes.⁴⁶ Pericyte deficiency is thought to cause BBB breakdown.⁵³ Thus, a decrease in pericyte population may not only affect the permeability of the BBB, allowing molecules that are normally filtered out to flow into the brain extracellular matrix, but also result in NVU.⁵⁴ Finally, pericytes have also been shown to maintain the integrity of cerebral blood vessels and serve a neuroprotective function.^{15,55,56}

fMRI of brain tumors

Most traditional magnetic resonance imaging (MRI) techniques for brain tumor imaging are geared toward elucidating angiogenesis-induced vascular remodeling⁵⁷⁻⁵⁹ and the changes brain tumors cause in the CNS microenvironment.⁶⁰ Many of these MRI approaches exploit the kinetics of contrast agents as they transit through the cerebrovasculature.⁶¹ Dynamic contrast-enhanced (DCE) and dynamic susceptibility contrast (DSC) MRI are examples of such techniques.^{62,63} Typically, baseline images are first acquired before the injection of a contrast agent, which is usually a gadolinium (Gd) chelate.^{64,65} The contrast agent is administered via a power injector and images are acquired during and after the injection.⁶⁶ On the first pass of the contrast agent in T2* DSC perfusion imaging, the arterial input function (AIF)⁶⁵ can be used to compute the cerebral blood volume (CBV), cerebral blood flow (CBF), and mean transit time (MTT) required for the clearance of the contrast agent through the vascular bed.⁶⁷⁻⁶⁹ On the other hand, T1 steady state DCE utilizes delayed imaging after the first pass of the contrast bolus primarily to measure permeability. These processes facilitate tumor localization and monitoring of locations with BBB breaching⁷⁰ and permit assessment of the angiogenic status of the tumor.⁷¹

Endogenous contrast-based MRI techniques such as arterial spin labeling (ASL) have also been successfully employed to characterize brain tumor-induced changes in the neurovasculature.^{72,73} ASL allows for perfusion quantification by using magnetically tagged arterial blood water protons as an intrinsic tracer. In this approach, the arterial blood water is magnetically tagged using radio frequency (RF) pulses that invert the bulk magnetization of water protons in the inflowing blood.⁷⁴ Baseline images are subtracted from the tagged images to detect hypo- and hyper-perfusion.⁷⁵

Clinically, ASL is particularly well-suited to measure CBF while DSC MRI is generally employed to measure CBV.

The above techniques work well for angiogenic vessels, particularly taking advantage of tumor vessels' characteristic changes in morphology and leakiness that cause edema and result in extravasation of the contrast agent or tagged molecules. However, these MRI techniques are unable to effectively detect vessel co-option, which unlike the angiogenic vessel phenotype does not involve hyperpermeable tumor vessels.^{23,34} Instead it involves the normal cerebrovasculature being hijacked by tufts of brain tumor cells at the early stages of tumor establishment.^{23,75} In this context, it can be challenging to determine the radiographic response of recurrent GBM to anti-angiogenic therapies⁷⁶ (discussed in the next section) with MRI due to possible pseudo-response, and the GBM switching to a more co-optive phenotype; both result in a lack of MR contrast enhancement.^{34,77}

Neurosurgeons rely on BOLD fMRI to map eloquent cortical regions. This is currently performed using task-based fMRI (tb-fMRI), although growing evidence suggests that resting state functional connectivity MRI (rs-fMRI) may serve as a complementary or alternative approach. All these measurements are made under the assumption that the change in CBF measured in response to a stimulus or task (e.g. fMRI) is directly correlated to neural firing within particular brain networks of interest,⁷⁸ or that the resting CBF is within the autoregulatory range (e.g. rs-fMRI) as can be seen with microvascular-scale optical imaging (Figure 3). However, recent studies have shown that brain tumors can cause varying degrees of NVU.^{47,79,80} Since fMRI measures perturbations in the CBF rather than neural activity directly, NVU has the potential to impair or decrease the BOLD response when mapping these crucial areas and therefore confound interpretation of clinical fMRI data.^{47,81,82} In a key study, Holodny et al. showed that enhancing portions of grade IV GBM demonstrated increases in rCBV as a result of neovascularization, and decreases in BOLD signal activation as a consequence of NVU.⁸³ Moreover, Pillai et al. found that NVU can occur even in low and intermediate grade gliomas (grades II and III).⁶ Therefore, traditional methods such as fMRI alone are unable to differentiate between BOLD signal attenuation due to NVU, or that due to a lack of neuronal response as GBMs progress.⁸² Pillai et al. proposed addressing this problem by using BOLD cerebrovascular reactivity (CVR) mapping during hypercapnia induction via breath-holding (BH CVR) in conjunction with task-based fMRI.⁸² Although exogenous CO₂ administration allows quantitative measurements of CVR, breath-holding can produce

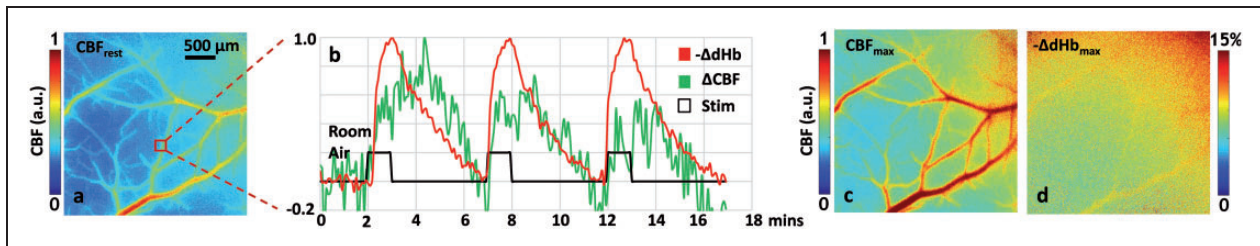


Figure 3. Imaging cerebral autoregulation at the microvascular spatial scale: Data from “microvascular-scale” in vivo optical imaging illustrating the autoregulatory hemodynamic response of the cerebrovasculature. (a) Laser speckle contrast (LSC) derived “baseline” or “resting” cerebral blood flow (CBF_{rest}) map computed from the average over the first 2 min during room air breathing. (b) Time courses illustrating relative in vivo changes in deoxyhemoglobin (red trace) and CBF (green trace) in response to carbogen (95% O_2 , 5% CO_2) inhalation. The carbogen inhalation (i.e. “Stim”) is shown as a solid black pulse train. The waveforms shown correspond to the 20×20 pixel ROI indicated by the red box in (a). Maps of (c) peak CBF response (CBF_{max}) and (d) the maximal change in deoxyhemoglobin ($-\Delta dHb_{max}$) in response to the carbogen challenge. Scale and color bars are shown where appropriate.

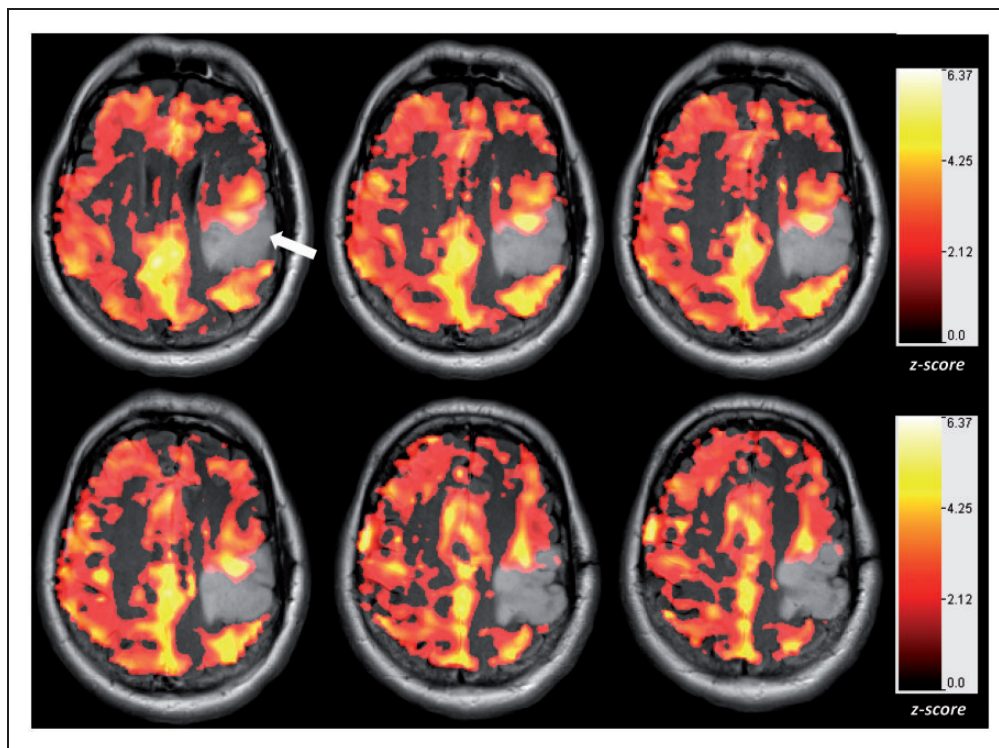


Figure 4. Neurovascular uncoupling in the tumor-affected brain hemisphere relative to the unaffected contralateral hemisphere: Cerebrovascular reactivity (CVR) maps overlaid on T2 FLAIR images obtained on a 7T MRI system during performance of a breath-hold task for a patient with a low-grade oligoastrocytoma (WHO grade II). The CVR maps were generated using a general linear model analysis in which the breath-hold hypercapnia state was contrasted with the baseline normal breathing blocks. Notice that within and in the immediate vicinity of the tumor, there is abnormally decreased and in some areas absent CVR (arrow) relative to the normal contralateral hemisphere. This is an indication of the presence of neurovascular uncoupling (NVU). All CVR maps were thresholded at a z-score > 1.0 .

similar results with less patient discomfort and less equipment setup time.⁸⁴ Breath-hold and other hypercapnia challenges (Figure 4) permit assessment of CBF and vasodilation in the absence of task-induced neuronal stimulation.⁸⁵ Impaired CVR can be an important

indicator of NVU.⁸⁵ Based on BH CVR and task-based BOLD fMRI mapping, patients with low grade tumors were found to have impaired sensorimotor activation on the side ipsilateral to the tumor as compared to the corresponding homologous area in the contralateral

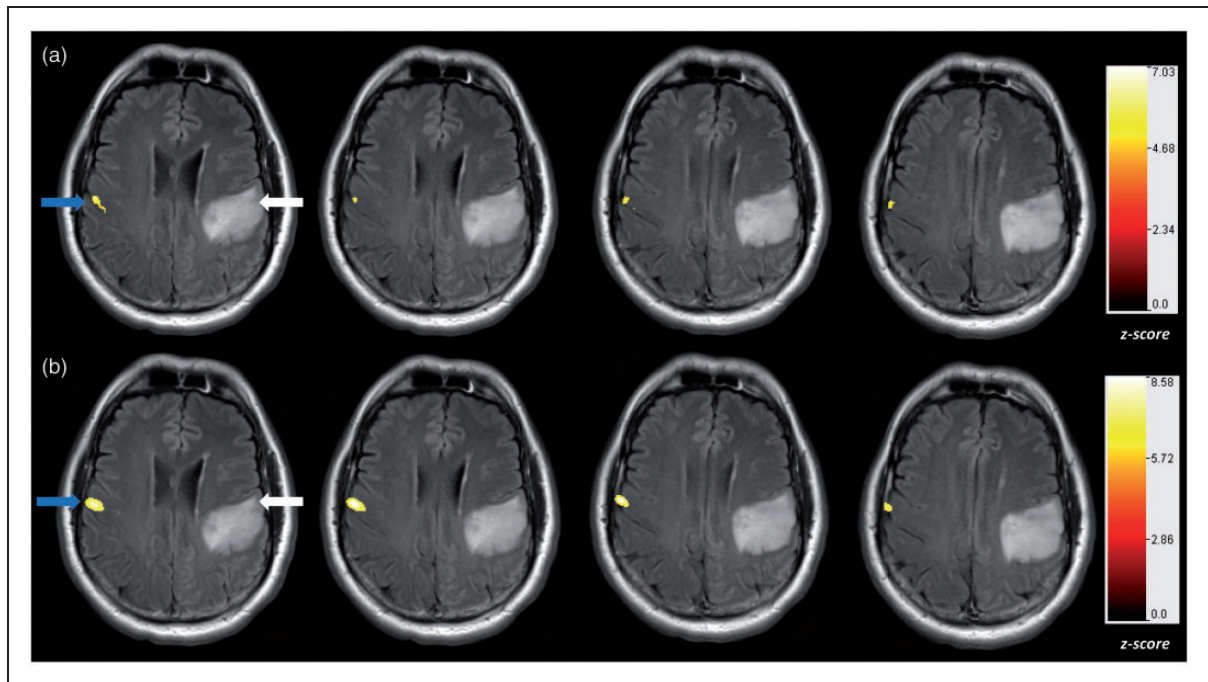


Figure 5. Neurovascular uncoupling in task-based and resting-state fMRI: A patient with a low-grade (WHO grade II) non-enhancing oligodendroglioma underwent fMRI at (a) 3T, and (b) ultra-high field 7T. Both fMRI maps were registered and overlaid on T2 FLAIR images. (a) Vertical tongue movement task activation map (blue arrow) at 3T thresholded at a z-score > 4.5. (b) The resting-state fMRI map displaying sensorimotor activation (blue arrow) derived from an independent component analysis (ICA) with order of 30, thresholded at z-score > 5.0. The white arrow points to the expected areas of sensorimotor cortex activation in all panels. Both task-based and resting-state fMRI methods demonstrated NVU.

hemisphere (Figure 4).⁸⁶ The attenuated BOLD response to tasks and the impaired CVR indicate NVU on the ipsilesional side since the patients did not display corresponding focal neurologic deficits.⁶ More recent studies from the Pillai lab have shown that these changes to the ipsilesional side were also observable with both task-based and resting-state fMRI in low-grade glioma patients (Figure 5). These results collectively suggest that NVU can pose problems for both task-based and resting-state clinical fMRI paradigms.^{47,86} These fMRI imaging techniques could facilitate tumor monitoring despite non-enhancing, co-optive growth of GBMs and facilitate the identification of potential areas wherein the fMRI signal may be compromised due to NVU. However, to make this feasible one needs to understand the interplay between the tumor vasculature, the BOLD contrast mechanism, and NVU detected at the microvascular scale. Recent preclinical studies from the Pathak laboratory are proposing to do just that.

For example, in a murine brain tumor model, we showed that the presence of brain tumors diminished BOLD signal fluctuations globally relative to healthy individuals. This suggested that mechanisms necessary for proper vasodilation were impaired even in regions unaffected by the physical modifications that occur

with NVU. In healthy mice, regions within the same hemisphere exhibited positive functional correlations, whereas contralateral functional connectivity was largely anti-correlated (Figure 6(b)). In brain tumor-bearing mice, this organization was lost, namely functional connectivity between all regions was distributed randomly with cross-correlations of roughly zero (Figure 6(a)). These resting-state changes in functional connectivity were found to be the result of neurovascular uncoupling as well as the mass effect of the progressing brain tumor. Overall evidence suggested that brain tumors exert a global rather than simply local effect on brain functional connectivity, and such global effects may explain cognitive deficits experienced by patients. Currently, our laboratory is investigating the interplay between brain tumor progression and NVU at microvascular spatial scales using *in vivo* optical imaging techniques (Figure 3).

It is worth noting that NVU not only disrupts functional connections between different brain regions but can also result in a loss of structural connectivity. Recent diffusion tensor imaging (DTI) studies have revealed the disruption of white matter tracts in tumorous regions in the brain.^{34,87,88} Thus, DTI is a promising complementary imaging method for characterizing the changes in structural connectivity that accompany

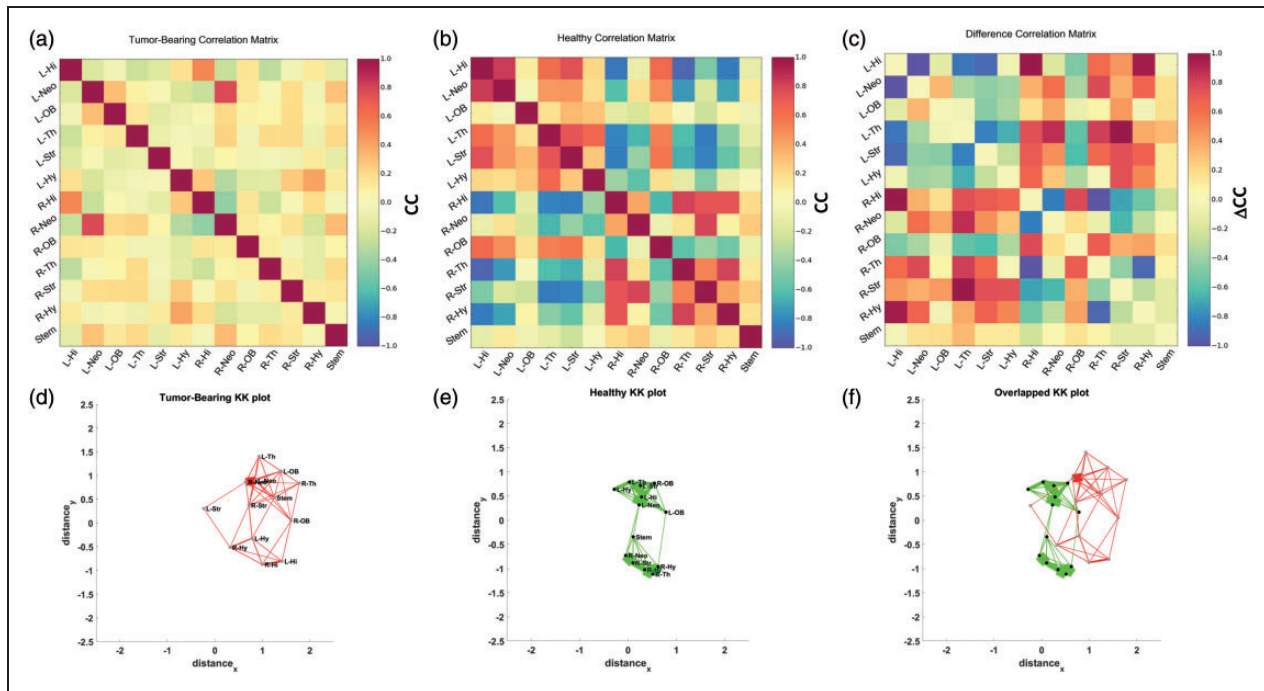


Figure 6. Brain tumors disrupt the normal inter- and intra-hemispheric resting-state functional connectivity due to neurovascular uncoupling: Correlation coefficient (CC) matrices illustrating the resting state functional connectivity for (a) regions-of-interest (ROI) from a 9L brain tumor-bearing mouse; (b) ROI from a healthy mouse. (c) The “difference” CC matrix between tumor-bearing and normal mouse ROIs illustrating the inter-ROI connectivity most affected by the presence of a tumor. To visually represent the resting state connectivity between murine brain regions, we generated force-directed spatial graphs using the Kamada-Kawai (KK) algorithm. In this spatial graph, each brain ROI was represented by a node and the strength of the connectivity between ROI represented by the thickness of the edge. The end result was a KK plot corresponding to the CC matrices in (a) and (b), respectively. (d) KK plot for a brain tumor-bearing mouse; (e) KK plot for a normal mouse. (f) Overlaying the KK-plots in (d) and (e) illustrates the alterations in resting state connectivity between tumor-bearing and normal brains. ROI labels have been omitted in (f) for clarity.

changes in functional connectivity with brain tumor progression.⁸⁹ With increasing utilization of more advanced diffusion methods such as diffusion spectrum imaging (DSI), diffusion kurtosis imaging (DKI), and high angular resolution diffusion imaging (HARDI), the complementary role of structural connectivity to functional connectivity is becoming more apparent and will need to be investigated in greater detail in the future in the setting of brain tumors.⁹⁰

Collectively, multi-modality imaging methods combining fMRI (both task-based and resting-state), CVR, and DTI/DSI could facilitate an improved understanding and monitoring of GBM progression despite neurovascular uncoupling and a phenotypic shift to co-optive growth. These techniques would eventually permit disentangling the effects of NVU from the absence of neural activity.

Implications for the use of fMRI as a biomarker of GBM progression

As discussed in the previous section, interpretation of clinical fMRI of brain tumor patients can be

confounded by the presence of NVU. The absence of an expected concomitant BOLD signal change in brain regions where NVU is present impedes extraction of information about neuronal activity. This deficiency of information is a major obstacle for assessing the effect of GBM on eloquent cortical areas, stratifying patients and evaluating potential new GBM treatments. Although task-based and resting state fMRI are routinely obtained in GBM patients for presurgical mapping and can provide complementary information regarding various brain networks, one needs to be mindful of tumor-related local and distant spatial effects on functional connectivity. Additionally, although we have shown in patients that both high- and low-grade gliomas can produce regional CVR impairment,^{6,85} the spatial resolution of CVR mapping is at the single voxel level, whereas glioma infiltration occurs on a more microscopic (i.e. sub-voxel) scale. In high grade gliomas, the NVU detected through regional CVR impairment is mostly related to decreased vascular reactivity secondary to tumor angiogenesis, while in lower grade gliomas, the NVU is likely related to other factors such as astrocytic, neurotransmitter, or pericyte

dysfunction. In high grade gliomas, the CVR abnormality often extends beyond the enhancing tumor portion. Therefore, CVR mapping can detect NVU in both areas of enhancing and non-enhancing tumor infiltration and research is underway in preclinical models to determine if it can also be used to detect tumor progression using vascular co-option.⁹¹

It still remains to be seen whether “normalizing” the brain tumor vasculature by suppressing growth of angiogenic vessels via antiangiogenic therapies can reverse the effects of NVU.⁹² If neurovascular coupling can be restored, tb-fMRI, rs-fMRI, and BH CVR mapping have potential to detect this recovery. Typically, antiangiogenic therapies target the new, immature, leaky vasculature, which is particularly useful when brain tumors are growing via the angiogenic pathway.⁹³ There are two common classes of anti-angiogenic agents that act on VEGF: anti-VEGF antibodies and VEGF-receptor tyrosine kinase inhibitors (TKIs).⁹³ Both have demonstrated an ability to reduce vessel leakage, decrease permeability of the BBB,^{93,94} and lessen edema.⁹⁵ As discussed previously, leaky vessels that cause edema and BBB disruption also result in an increase in interstitial fluid pressure (IFP). High IFP presents an obstacle to drug uptake, so anti-angiogenic therapies also offer the possibility of enhanced drug delivery in brain tumors.⁹⁶ Optical,⁹⁷ MRI,⁹⁸ and other imaging techniques are currently being employed to evaluate the effects of these new therapies, including the possibility of restoring neurovascular coupling. Tumor volume in traditional contrast-enhanced MRI scans appears to be reduced with anti-angiogenic therapy, but this may be simply the result of a pseudo-response with lessened vascular leakage and contrast agent extravasation rather than a reduction in tumor burden.⁹⁹ These factors must be disentangled before conclusions can be drawn about the efficacy of these treatments.

Unfortunately, sustained antiangiogenic therapy can also encourage brain tumors to switch from an angiogenic to a co-optive growth pattern.¹⁰⁰ The latter is more difficult to detect radiologically with MRI as well as to treat, since the host vasculature stays mostly intact.³⁴ Typically, only serial conventional T2/FLAIR MRI evaluation over months enables delayed confirmation of such progression via a co-optive growth pattern. Furthermore, activation of alternative angiogenic pathways, hypoxia-induced increases in angiogenic signaling molecules, and recruitment of stem cells also result in resistance to anti-angiogenic therapy.^{101,102} Therefore, there is an exigent need to identify more specific and sensitive fMRI-based biomarkers that can track GBM growth and possible restoration of neurovascular coupling after anti-angiogenic therapy. Breath-hold CVR mapping has the potential to be such a technique.

Alternatively, exogenous gas administration could also be used for CVR assessment, but this is more difficult in clinical settings due to the need for specialized equipment and greater patient discomfort associated with this approach. As we have shown in animal models,⁹¹ rs-fMRI may also be used for this purpose, but its clinical use in this context has not been as widely adopted. Finally, it is crucial to validate and qualify these new fMRI-biomarkers, so that they can cross the “translational-gap” and satisfy the imaging biomarker roadmap for cancer studies as defined by international consensus.¹⁰³

Conclusion

Gliomas result in varying degrees of perturbation to the neurovascular unit composed of astrocytes, pericytes, and endothelial cells. These disruptions impair neurovascular coupling and can lead to faster excitotoxicity due to the lack of vascular response and an inability to supply metabolites and oxygen to active neuronal populations. The resulting hypoxia in conjunction with tumor cell death eventually triggers a cascade of events that leads to angiogenic growth and poorly formed vasculature to support tumor growth. A shift to the co-optive phenotype, in which glioma cells take over control of host vascular tone, can also occur in patients.

Recent studies have shown that neurovascular uncoupling to varying degrees accompanies GBM, and can confound fMRI interpretations in the setting of brain tumor progression and presurgical mapping. New methods are being developed for these cases that include combinations of BOLD fMRI, BH CVR, and DTI. Although these complementary imaging methods exhibit potential as biomarkers, more work must be done to integrate these techniques into the clinical workflow and make their interpretation clearer in the presence of NVU. If successful, these techniques would enable us to monitor not only CBF changes and vascular response, but also alterations in structural and functional connectivity. Together these methods would pave the way to better understanding GBM progression, angiogenic and co-optive growth and facilitate the development of new therapies for GBM. Finally, combining these complementary approaches with traditional contrast-enhanced MRI methods would enable us to better evaluate the efficacy of anti-angiogenic therapies and their ability to restore neurovascular coupling, and re-establish cortical function in GBM-infiltrated brain regions.

Funding

The author(s) disclosed receipt of the following financial support for the research, authorship, and/or publication of this

article: NCI 1R21CA175784-01 (APP), 1R01CA196701-01 (APP), and 2 R42 CA173976-02 (JJP).

Declaration of conflicting interests

The author(s) declared no potential conflicts of interest with respect to the research, authorship, and/or publication of this article.

References

1. Metea MR and Newman EA. Glial cells dilate and constrict blood vessels: a mechanism of neurovascular coupling. *J Neurosci* 2006; 26: 2862–2870.
2. Roy CS and Sherrington CS. On the regulation of the blood-supply of the brain. *J Physiol* 1890; 11: 85–158 17.
3. Hoge RD, Atkinson J, Gill B, et al. Linear coupling between cerebral blood flow and oxygen consumption in activated human cortex. *Proc Natl Acad Sci USA* 1999; 96: 9403–9408.
4. Logothetis NK and Wandell BA. Interpreting the BOLD signal. *Annu Rev Physiol* 2004; 66: 735–769.
5. Biswal B, Yetkin FZ, Haughton VM, et al. Functional connectivity in the motor cortex of resting human brain using echo-planar MRI. *Magn Reson Med* 1995; 34: 537–541.
6. Pillai JJ and Zaca D. Clinical utility of cerebrovascular reactivity mapping in patients with low grade gliomas. *World J Clin Oncol* 2011; 2: 397–403.
7. Araque A, Carmignoto G and Haydon PG. Dynamic signaling between astrocytes and neurons. *Annu Rev Physiol* 2001; 63: 795–813.
8. Navarrete M and Araque A. The Cajal school and the physiological role of astrocytes: a way of thinking. *Front Neuroanat* 2014; 8: 1–5.
9. Iadecola C and Nedergaard M. Glial regulation of the cerebral microvasculature. *Nat Neurosci* 2007; 10: 1369–1376.
10. Kimelberg HK and Nedergaard M. Functions of astrocytes and their potential as therapeutic targets. *Neurotherapeutics* 2010; 7: 338–353.
11. Watkins S, Robel S, Kimbrough IF, et al. Disruption of astrocyte-vascular coupling and the blood-brain barrier by invading glioma cells. *Nat Commun* 2014; 5: 1–15.
12. Huneau C, Benali H and Chabriat H. Investigating human neurovascular coupling using functional neuroimaging: A critical review of dynamic models. *Front Neurosci* 2015; 9: 1–12.
13. Abbott NJ, Patabendige AA, Dolman DE, et al. Structure and function of the blood-brain barrier. *Neurobiol Dis* 2010; 37: 13–25.
14. Lee J, Lund-Smith C, Borboa A, et al. Glioma-induced remodeling of the neurovascular unit. *Brain Res* 2009; 1288: 125–134.
15. Winkler EA, Bell RD and Zlokovic BV. Central nervous system pericytes in health and disease. *Nat Neurosci* 2011; 14: 1398–1405.
16. Daneman R, Zhou L, Kebede AA, et al. Pericytes are required for blood-brain barrier integrity during embryogenesis. *Nature* 2010; 468: 562–566.
17. Lebrin F, Deckers M, Bertolino P, et al. TGF-beta receptor function in the endothelium. *Cardiovasc Res* 2005; 65: 599–608.
18. Chen BR, Kozberg MG, Bouchard MB, et al. A critical role for the vascular endothelium in functional neurovascular coupling in the brain. *J Am Heart Assoc* 2014; 3: e000787.
19. Howitt L, Chaston DJ, Sandow SL, et al. Spreading vasodilatation in the murine microcirculation: attenuation by oxidative stress-induced change in electromechanical coupling. *J Physiol* 2013; 591: 2157–2173.
20. Tallini YN, Brekke JF, Shui B, et al. Propagated endothelial Ca²⁺ waves and arteriolar dilation in vivo: measurements in Cx40BAC GCaMP2 transgenic mice. *Circ Res* 2007; 101: 1300–1309.
21. Iliff JJ, Wang M, Liao Y, et al. A paravascular pathway facilitates CSF flow through the brain parenchyma and the clearance of interstitial solutes, including amyloid beta. *Sci Transl Med* 2012; 4: 147ra11.
22. Simon MJ and Iliff JJ. Regulation of cerebrospinal fluid (CSF) flow in neurodegenerative, neurovascular and neuroinflammatory disease. *Biochim Biophys Acta* 2016; 1862: 442–451.
23. Holash J, Maisonpierre PC, Compton D, et al. Vessel cooption, regression, and growth in tumors mediated by angiopoietins and VEGF. *Science (New York, NY)* 1999; 284: 1994–1998.
24. Folkman J. Tumor angiogenesis: therapeutic implications. *N Engl J Med* 1971; 285: 1182–1186.
25. Hardee ME and Zagzag D. Mechanisms of glioma-associated neovascularization. *Am J Pathol* 2012; 181: 1126–1141.
26. Maisonpierre PC, Suri C, Jones PF, et al. Angiopoietin-2, a natural antagonist for Tie2 that disrupts in vivo angiogenesis. *Science* 1997; 277: 55–60.
27. Zagzag D, Amirnovin R, Greco MA, et al. Vascular apoptosis and involution in gliomas precede neovascularization: a novel concept for glioma growth and angiogenesis. *Lab Invest* 2000; 80: 837–849.
28. Hardee ME and Zagzag D. Mechanisms of glioma-associated neovascularization. *Am J Pathol* 2012; 181: 1126–1141.
29. Kim H, Li Q, Hempstead BL, et al. Paracrine and autocrine functions of brain-derived neurotrophic factor (BDNF) and nerve growth factor (NGF) in brain-derived endothelial cells. *J Biol Chem* 2004; 279: 33538–33546.
30. Louissaint A Jr., Rao S, Leventhal C, et al. Coordinated interaction of neurogenesis and angiogenesis in the adult songbird brain. *Neuron* 2002; 34: 945–960.
31. Fagiani E and Christofori G. Angiopoietins in angiogenesis. *Cancer Lett* 2013; 328: 18–26.
32. Reiss Y, Machein MR and Plate KH. The role of angiopoietins during angiogenesis in gliomas. *Brain Pathol* 2006; 15: 311–317.
33. Jain RK, Tong RT and Munn LL. Effect of vascular normalization by antiangiogenic therapy on interstitial hypertension, peritumor edema, and lymphatic metastasis: insights from a mathematical model. *Cancer Res* 2007; 67: 2729–2735.

34. Jain RK, di Tomaso E, Duda DG, et al. Angiogenesis in brain tumours. *Nat Rev Neurosci* 2007; 8: 610–622.
35. Boucher Y, Salehi H, Witwer B, et al. Interstitial fluid pressure in intracranial tumours in patients and in rodents. *Br J Cancer* 1997; 75: 829–836.
36. Jain RK. Barriers to drug delivery in solid tumors. *Sci Am* 1994; 271: 58–65.
37. Monajati A and Heggeness L. Patterns of edema in tumors vs. infarcts: visualization of white matter pathways. *AJNR Am J Neuroradiol* 1982; 3: 251–255.
38. Du R, Lu KV, Petritsch C, et al. HIF1 α induces the recruitment of bone marrow-derived vascular modulatory cells to regulate tumor angiogenesis and invasion. *Cancer Cell* 2008; 13: 206–220.
39. Liebelt BD, Shingu T, Zhou X, et al. Glioma stem cells: signaling, microenvironment, and therapy. *Stem Cells Int* 2016; 2016: 7849890.
40. Zacchigna S, Lambrechts D and Carmeliet P. Neurovascular signalling defects in neurodegeneration. *Nat Rev Neurosci* 2008; 9: 169–181.
41. Sun Y, Jin K, Xie L, et al. VEGF-induced neuroprotection, neurogenesis, and angiogenesis after focal cerebral ischemia. *J Clin Invest* 2003; 111: 1843–1851.
42. Wang Y, Jin K, Mao XO, et al. VEGF-overexpressing transgenic mice show enhanced post-ischemic neurogenesis and neuromigration. *J Neurosci Res* 2007; 85: 740–747.
43. Jhaveri N, Chen TC and Hofman FM. Tumor vasculature and glioma stem cells: Contributions to glioma progression. *Cancer Lett* 2016; 380: 545–551.
44. Nagy JA, Chang SH, Shih SC, et al. Heterogeneity of the tumor vasculature. *Semin Thromb Hemost* 2010; 36: 321–331.
45. Patan S, Tanda S, Roberge S, et al. Vascular morphogenesis and remodeling in a human tumor xenograft: blood vessel formation and growth after ovariectomy and tumor implantation. *Circ Res* 2001; 89: 732–739.
46. Stanimirovic DB and Friedman A. Pathophysiology of the neurovascular unit: disease cause or consequence? *J Cereb Blood Flow Metab* 2012; 32: 1207–1221.
47. Agarwal S, Sair HI, Yahyavi-Firouz-Abadi N, et al. Neurovascular uncoupling in resting state fMRI demonstrated in patients with primary brain gliomas. *J Magn Reson Imaging* 2016; 43: 620–626.
48. Warth A, Kroger S and Wolburg H. Redistribution of aquaporin-4 in human glioblastoma correlates with loss of agrin immunoreactivity from brain capillary basal laminae. *Acta Neuropathol* 2004; 107: 311–318.
49. Hatton JD and Sang UH. Orthogonal arrays are absent from the membranes of human glioblastomatous tissues. *Acta Anat (Basel)* 1990; 137: 363–366.
50. Warth A, Mittelbronn M and Wolburg H. Redistribution of the water channel protein aquaporin-4 and the K⁺ channel protein Kir4.1 differs in low- and high-grade human brain tumors. *Acta Neuropathol* 2005; 109: 418–426.
51. Azad TD, Pan J, Connolly ID, et al. Therapeutic strategies to improve drug delivery across the blood-brain barrier. *Neurosurg Focus* 2015; 38: E9.
52. Liebner S, Fischmann A, Rascher G, et al. Claudin-1 and claudin-5 expression and tight junction morphology are altered in blood vessels of human glioblastoma multiforme. *Acta Neuropathol* 2000; 100: 323–331.
53. Takata F, Dohgu S, Matsumoto J, et al. Brain pericytes among cells constituting the blood-brain barrier are highly sensitive to tumor necrosis factor- α , releasing matrix metalloproteinase-9 and migrating in vitro. *J Neuroinflammation* 2011; 8: 1–12.
54. Hamilton NB, Attwell D and Hall CN. Pericyte-mediated regulation of capillary diameter: a component of neurovascular coupling in health and disease. *Front Neuroenergetics* 2010; 2: 1–14.
55. Armulik A, Genove G, Mae M, et al. Pericytes regulate the blood-brain barrier. *Nature* 2010; 468: 557–561.
56. Bell RD, Winkler EA, Sagare AP, et al. Pericytes control key neurovascular functions and neuronal phenotype in the adult brain and during brain aging. *Neuron* 2010; 68: 409–427.
57. Emblem KE, Farrar CT, Gerstner ER, et al. Vessel caliber—a potential MRI biomarker of tumour response in clinical trials. *Nat Rev Clin Oncol* 2014; 11: 566–584.
58. Kim E, Cebulla J, Ward BD, et al. Assessing breast cancer angiogenesis in vivo: which susceptibility contrast MRI biomarkers are relevant? *Magn Reson Med* 2013; 70: 1106–1116.
59. Pathak AP, Hochfeld WE, Goodman SL, et al. Circulating and imaging markers for angiogenesis. *Angiogenesis* 2008; 11: 321–335.
60. Peet AC, Arvanitis TN, Leach MO, et al. Functional imaging in adult and paediatric brain tumours. *Nat Rev Clin Oncol* 2012; 9: 700–711.
61. Tofts PS, Brix G, Buckley DL, et al. Estimating kinetic parameters from dynamic contrast-enhanced t1-weighted MRI of a diffusible tracer: Standardized quantities and symbols. *J Magn Reson Imag* 1999; 10: 223–232.
62. Choyke PL, Dwyer AJ and Knopp MV. Functional tumor imaging with dynamic contrast-enhanced magnetic resonance imaging. *J Magn Reson Imaging* 2003; 17: 509–520.
63. Quarles CC, Gore JC, Xu L, et al. Comparison of dual-echo DSC-MRI- and DCE-MRI-derived contrast agent kinetic parameters. *Magn Reson Imaging* 2012; 30: 944–953.
64. Moseley ME, Vexler Z, Asgari HS, et al. Comparison of Gd- and Dy-chelates for T2 contrast-enhanced imaging. *Magn Reson Med* 1991; 22: 259–264; discussion 65–67.
65. O'Connor JP, Tofts PS, Miles KA, et al. Dynamic contrast-enhanced imaging techniques: CT and MRI. *Br J Radiol* 2011; 84 Spec No 2: S112–S120.
66. Jackson A, Buckley DL and Parker GJM. *Dynamic contrast-enhanced magnetic resonance imaging in oncology (Medical Radiology/Diagnostic Imaging)*. Berlin, Heidelberg: Springer-Verlag, 2005.
67. Ostergaard L, Weisskoff RM, Chesler DA, et al. High resolution measurement of cerebral blood flow using intravascular tracer bolus passages. Part I: Mathematical approach and statistical analysis. *Magn Reson Med* 1996; 36: 715–725.

68. Rosen BR, Belliveau JW, Buchbinder BR, et al. Contrast agents and cerebral hemodynamics. *Magn Reson Med* 1991; 19: 285–292.
69. Weisskoff RM, Chesler D, Boxerman JL, et al. Pitfalls in MR measurement of tissue blood flow with intravascular tracers: which mean transit time? *Magn Reson Med* 1993; 29: 553–558.
70. Tofts PS and Kermode AG. Measurement of the blood-brain-barrier permeability and leakage space using dynamic MR imaging: 1. Fundamental concepts. *Magn Reson Med* 1991; 17: 357–367.
71. Donahue KM, Krouwer HG, Rand SD, et al. Utility of simultaneously acquired gradient-echo and spin-echo cerebral blood volume and morphology maps in brain tumor patients. *Magn Reson Med* 2000; 43: 845–853.
72. Moffat BA, Chenevert TL, Hall DE, et al. Continuous arterial spin labeling using a train of adiabatic inversion pulses. *J Magn Reson Imaging* 2005; 21: 290–296.
73. Pollock JM, Tan H, Kraft RA, et al. Arterial spin-labeled MR perfusion imaging: clinical applications. *Magn Reson Imaging Clin N Am* 2009; 17: 315–338.
74. Petcharunpaisan S, Ramalho J and Castillo M. Arterial spin labeling in neuroimaging. *World J Radiol* 2010; 2: 384–398.
75. Donnem T, Hu J, Ferguson M, et al. Vessel co-option in primary human tumors and metastases: an obstacle to effective anti-angiogenic treatment? *Cancer Med* 2013; 2: 427–436.
76. Zuniga RM, Torcuator R, Doyle T, et al. Retrospective analysis of patterns of recurrence seen on MRI in patients with recurrent glioblastoma multiforme treated with bevacizumab plus irinotecan. *J Clin Oncol* 2008; 26: 13013.
77. Caspani EM, Crossley PH, Redondo-Garcia C, et al. Glioblastoma: a pathogenic crosstalk between tumor cells and pericytes. *PLoS One* 2014; 9: e101402.
78. Maldjian JA, Schulder M, Liu WC, et al. Intraoperative functional MRI using a real-time neurosurgical navigation system. *J Comput Assist Tomogr* 1997; 21: 910–912.
79. Atlas SW, Howard RS II, Maldjian J, et al. Functional magnetic resonance imaging of regional brain activity in patients with intracerebral gliomas: findings and implications for clinical management. *Neurosurgery* 1996; 38: 329–338.
80. Holodny AI, Schulder M, Liu WC, et al. The effect of brain tumors on BOLD functional MR imaging activation in the adjacent motor cortex: implications for image-guided neurosurgery. *AJNR Am J Neuroradiol* 2000; 21: 1415–1422.
81. Holodny AI, Schulder M, Liu WC, et al. Decreased BOLD functional MR activation of the motor and sensory cortices adjacent to a glioblastoma multiforme: implications for image-guided neurosurgery. *AJNR Am J Neuroradiol* 1999; 20: 609–612.
82. Zaca D, Jovicich J, Nadar SR, et al. Cerebrovascular reactivity mapping in patients with low grade gliomas undergoing presurgical sensorimotor mapping with BOLD fMRI. *J Magn Reson Imaging* 2014; 40: 383–390.
83. Hou BL, Bradbury M, Peck KK, et al. Effect of brain tumor neovasculature defined by rCBV on BOLD fMRI activation volume in the primary motor cortex. *Neuroimage* 2006; 32: 489–497.
84. Pillai JJ and Mikulis DJ. Cerebrovascular reactivity mapping: an evolving standard for clinical functional imaging. *AJNR Am J Neuroradiol* 2015; 36: 7–13.
85. Pillai JJ and Zaca D. Comparison of BOLD cerebrovascular reactivity mapping and DSC MR perfusion imaging for prediction of neurovascular uncoupling potential in brain tumors. *Technol Cancer Res Treat* 2012; 11: 361–374.
86. Agarwal S, Sair HI, Airan R, et al. Demonstration of brain tumor-induced neurovascular uncoupling in resting-state fMRI at ultrahigh field. *Brain Connect* 2016; 6: 267–272.
87. Lu S, Ahn D, Johnson G, et al. Peritumoral diffusion tensor imaging of high-grade gliomas and metastatic brain tumors. *AJNR Am J Neuroradiol* 2003; 24: 937–941.
88. Pathak AP, Kim E, Zhang J, et al. Three-dimensional imaging of the mouse neurovasculature with magnetic resonance microscopy. *PLoS One* 2011; 6: e22643.
89. LaViolette PS, Mickevicius NJ, Cochran EJ, et al. Precise ex vivo histological validation of heightened cellularity and diffusion-restricted necrosis in regions of dark apparent diffusion coefficient in 7 cases of high-grade glioma. *Neuro Oncol* 2014; 16: 1599–1606.
90. Chamberland M, Bernier M, Fortin D, et al. 3D interactive tractography-informed resting-state fMRI connectivity. *Front Neurosci* 2015; 9: 1–15.
91. Senarathna J, Hadjiabadi D, Batra D, et al. Wide area mapping of resting state functional connectivity at microvascular resolution with multi-contrast optical imaging. In: *SPIE photonics West BIOS*, San Francisco, CA, 2017, p.148.
92. Jain RK. Normalizing tumor vasculature with anti-angiogenic therapy: a new paradigm for combination therapy. *Nat Med* 2001; 7: 987–989.
93. Lu-Emerson C, Duda DG, Emblem KE, et al. Lessons from anti-vascular endothelial growth factor and anti-vascular endothelial growth factor receptor trials in patients with glioblastoma. *J Clin Oncol* 2015; 33: 1197–1213.
94. Goel S, Wong AH and Jain RK. Vascular normalization as a therapeutic strategy for malignant and nonmalignant disease. *Cold Spring Harb Perspect Med* 2012; 2: a006486.
95. Jain RK. Lessons from multidisciplinary translational trials on anti-angiogenic therapy of cancer. *Nat Rev Cancer* 2008; 8: 309–316.
96. Lunt SJ, Fyles A, Hill RP, et al. Interstitial fluid pressure in tumors: therapeutic barrier and biomarker of angiogenesis. *Future Oncol* 2008; 4: 793–802.
97. Sanai N, Eschbacher J, Hattendorf G, et al. Intraoperative confocal microscopy for brain tumors: a feasibility analysis in humans. *Neurosurgery* 2011; 68: 282–290; discussion 90.
98. Sorensen AG, Batchelor TT, Zhang WT, et al. A “vascular normalization index” as potential mechanistic biomarker to predict survival after a single dose of cediranib in recurrent glioblastoma patients. *Cancer Res* 2009; 69: 5296–5300.

99. van den Bent MJ, Vogelbaum MA, Wen PY, et al. End point assessment in gliomas: novel treatments limit usefulness of classical Macdonald's Criteria. *J Clin Oncol* 2009; 27: 2905–2908.
100. Rubenstein JL, Kim J, Ozawa T, et al. Anti-VEGF antibody treatment of glioblastoma prolongs survival but results in increased vascular cooption. *Neoplasia* 2000; 2: 306–314.
101. Bergers G and Hanahan D. Modes of resistance to anti-angiogenic therapy. *Nat Rev Cancer* 2008; 8: 592–603.
102. Giuliano S and Pages G. Mechanisms of resistance to anti-angiogenesis therapies. *Biochimie* 2013; 95: 1110–1119.
103. O'Connor JP, Aboagye EO, Adams JE, et al. Imaging biomarker roadmap for cancer studies. *Nat Rev Clin Oncol* 2017; 14: 169–186.